Clinorotation affects myotube formation through fluid motions instead of simulated microgravity

Janet Mansour[1,*], Carolin Berwanger[1,2,*], Marcel Jung[1,§], Ludwig Eichinger[3], Ben Fabry[4], Christoph S. Clemen[1,2,#]

[1] Institute of Aerospace Medicine, German Aerospace Center (DLR), Cologne, Germany

[2] Institute of Vegetative Physiology, Medical Faculty, University of Cologne, Cologne, Germany

[3] Institute of Biochemistry I, Medical Faculty, University of Cologne, Cologne, Germany

[4] Biophysics Group, Department of Physics, Friedrich-Alexander University Erlangen-Nürnberg, Erlangen, Germany

*These two first authors contributed equally to this work.

[§]Present address: Institute for Experimental Immunology and Imaging, University Hospital Essen, University of Duisburg-Essen, Essen, Germany

[#]Author for correspondence:

Christoph S. Clemen, Institute of Aerospace Medicine, German Aerospace Center (DLR), Linder Höhe, 51147 Cologne, Germany; Phone: +49 2203 601 3468; christoph.clemen@dlr.de; christoph.clemen@uni-koeln.de

Abstract

To study processes related to weightlessness in ground-based cell biological research, a theoretical microgravity environment is typically simulated with a clinostat – a small laboratory device that rotates cell culture vessels with the aim to average-out the vector of gravitational forces. Here, we report that these rotational movements induce complex fluid motions in the cell culture vessel that can trigger unintended cellular responses. Specifically, we demonstrate that suppression of myotube formation by 2D-clino-rotation is not an effect of the assumed microgravity but instead is a consequence of fluid motion. Therefore, cell biological results from clino-rotation cannot be attributed to microgravity unless alternative explanations have been rigorously tested and ruled out. In this setting we consider the inclusion of at least two control experiments as mandatory, i) a static, non-rotating control, and ii) controls for fluid motion. Finally, we discuss strategies to minimize fluid motion in clino-rotation experiments.

Keywords

Simulated microgravity; clinostat; gravity; fluid flow; fluid motion; myoblasts; myotubes; mammalian cell culture; shear force; shear stress

Introduction

'Simulated microgravity' (Herranz et al., 2013) is the technical term for a ground-based laboratory condition used as a workaround for the conduction of experiments that otherwise have to be carried out under real microgravity conditions in space. For gravity-related cell biological research, 2D-clinostats, rotating wall vessels, 3D-clinostats, random positioning machines, and magnetic levitation devices have been developed (Brungs et al., 2016; Calvaruso et al., 2021; Hasenstein, 2022; Herranz et al., 2013; Klaus, 2001; Zhang et al., 2022). Often used, because of its simple construction, is the 2D-clinostat, where cells are cultured on a flat, horizontal surface that is rotated around an in-plane axis. Cells grown along or close to the horizontal rotation axis experience negligible centrifugal forces but are subjected to a permanently changing gravitational force vector direction that averages-out to zero. Although the rotating cells still experience the same magnitude of gravitational forces, this approach is widely considered as a microgravity-analogue to conditions in space/earth orbit where the gravitational forces are balanced by centrifugal forces (Briegleb, 1992; Brungs et al., 2016; Hauslage et al., 2017; Herranz et al., 2013; Zhang et al., 2022).

Because cellular adaptation to external forces can be rapid, the rotation speed of the clinostat must be sufficiently fast. A speed of 60 rpm was reported to be the most effective setting for a functional microgravity simulation (Briegleb, 1992; Brungs et al., 2016; Herranz et al., 2013). For such experiments, adherent mammalian cells are typically seeded onto standard plastic cell culture vessels, e.g., 'slide flasks' (#170920; Nunc/Thermo Scientific, Waltham, USA), that are completely filled with equilibrated medium, carefully sealed, and attached to a clinostat that rotates the vessels along the horizontal axis (Eiermann et al., 2013).

In the present work, murine myoblasts (C2C12 cells, ECACC 91031101) were seeded onto the slides of slide flasks. After one day the growth medium was replaced by a differentiation medium and the flasks were attached to a 60 rpm-rotating 2D-slide flask-clinostat. Myotube formation was monitored over a time period of typically seven days. We found that clino-rotation suppressed myotube formation, in agreement with previous work reporting reduced number of myotubes near the centre of rotation as well as myofibrillar changes with aberrant filamin-C and α-actinin staining patterns within these cells

(Mansour Jamaleddine, 2021). The present study, however, demonstrates that this effect cannot be attributed to the simulated microgravity conditions. Instead, we show that the cellular responses are dominated by rotation-induced fluid motion of the cell culture medium. This finding suggests that the previously reported responses of mammalian cells in liquid culture in assumed simulated microgravity obtained using clinostats may have been similarly dominated by rotation-induced fluid motion. We discuss strategies for improving the design of clinostats to minimize such fluid motion in future cell biological studies.

Results

Myotube suppression during clino-rotation does not depend on simulated microgravity

With the intention of studying effects of mechanical unloading on muscle cells, we performed 2D-clino-rotation assays with differentiating C2C12 myoblasts over prolonged time periods (Fig. 1A-C). Visual inspection of the slide flasks by phase contrast microscopy after six to eight days of differentiation consistently showed suppressed myotube formation within an approximately 4 mm wide band without sharp limitation, which was visible along the rotational axis across the entire slide (Fig. 1D). Myotubes grown as a control on static, non-rotating slides did not show a reduced density along the centerline of the slide but a virtually even formation of myotubes (Fig. 1F). This result initially was interpreted as being related to the skeletal muscle tissue loss observed under microgravity conditions in space (Rittweger et al., 2018), presumably because a sufficient microgravity environment has been generated near the rotational axis, while microgravity conditions outside this narrow band break down due to above-threshold centrifugal forces as described previously (Eiermann et al., 2013).

To test the validity of the latter assumption, we mounted the slide 4 mm above the rotational axis, which exposes all the adherent cells to above-threshold centrifugal forces of 0.016 RCF (Fig. 1B). Notably, this offset-rotation also led to significantly suppressed myotube formation, again within a 4 mm band along the rotational axis (Fig. 1E), a finding that cannot be found in the controls (Fig. 1F). The static, non-rotating controls were placed on top of the clinostat to expose the cells to the same vibrational forces (Fig. 1A). Indeed, quantitation of the number of myotubes in microscopic field of views within the 4 mm bands showed no significant difference between clino-rotation (median count 35) and offset-rotation (median count 36), while the numbers of myotubes from these two conditions were significantly lower as compared to those of the static, non-rotating control (median count 59) (Fig. 1G). Additional quantitation of the widths of these myotubes revealed statistically significant differences between groups (Fig. 1H), but the marginal differences (median widths 17, 15, and 14 µm),

although they were statistically significant, can rather not be considered a biologically relevant effect. Together, the results of the clino- and offset-rotation experiments strongly suggest that the reduced myotube density along a central band near the rotational axis is not caused by a break-down of microgravity conditions outside this band but instead must have been due to previously unexplored effects. Ultimately, the suppression of myotube formation by such effects during clino-rotation would have been incorrectly attributed to simulated microgravity and thus misinterpreted.

Fluid motion markedly influences C2C12 myotube formation

Based on studies that reported rotation-induced motion of the cell culture medium in flasks mounted to a 3D-clinostat (two-frame rotation) (Wüest et al., 2015; Wüest et al., 2017; Zhang et al., 2022), we reasoned that such fluid motion might influence differentiation of myoblasts into myotubes. The effect could be for example due to small shear forces or fluid convection that disturbs the local concentration profile of secreted auto- or paracrine differentiation signals, also in our 2D-clinostat. To test this hypothesis, we added different amounts of polystyrene beads of 140, 250 or 500 µm diameter as tracer particles to medium-filled 2D-clino-rotating slide flasks (Fig. 2A), and connected a mini-camera to a slide flask filled with culture medium and tracer particles, and let them rotate together (Fig. 3A).

These experiments revealed the presence of fluid motion to a considerable extent. Observation of the entirety of particles as well as tracking of individual particles in different zones of the rotating slide flask revealed a complex pattern of flow directions and velocities during the steady-state phase of 2D-clino-rotation (Fig. 3B). Essential for cells adherent to the slide is their permanent exposure to the slow linear and cylindrical fluid motions. Close to the cells (100 to 250 µm distance), we observed velocities of particles in a range of 2.7 to 6.5 mm/s, corresponding to tangential shear forces on the adherent, differentiating myoblasts of around 15 to 25 mPa, assuming a viscosity of the culture medium of 1 mPa s and a linear decrease of the fluid flow velocity from the particle to the cell surface (no-slip condition). It has been shown that such forces cause significant cellular responses in e.g., human primary osteoblastic cells already at ≈60 µPa (Liegibel et al., 2004), human primary cerebral cortex astrocytes at >50 mPa (Khodadadei et al., 2021), murine primary cortical astrocytes at 25 mPa (Wakida et al., 2020), or C8-D1A murine cerebellar astrocytes (ATCC CRL-2541) at only 3 mPa (Lee et al., 2020). Therefore, the observed suppression of C2C12 myotube formation in a narrow region along the rotational axis may be attributed to shear stress.

To test next if fluid motion influences myotube formation, we modified the slide flasks and added a fluid inlet and outlet along the end faces (Fig. 2B). We then perfused the 'flow flasks' using a peristaltic pump with equilibrated (5% CO_2, 37°C) differentiation medium at average flow rates of 57 µL/min,

570 µL/min, and 5.7 mL/min. A flow rate of 5.7 mL/min (equivalent average flow speed of 0.24 mm/s), the fluid shear stress at the cell layer is estimated to be 95 µPa, completely suppressed myotube formation and also caused accumulation of cell debris (Fig. 2D). Likewise, flow rates of 570 µL/min (0.024 mm/s, 9.5 µPa) and even 57 µL/min (0.0024 mm/s, 0.9 µPa) markedly inhibited myotube formation (Fig. 2E, F).

In separate experiments, we placed slide flasks with differentiating myoblasts on a 5°-tilt-angle rocking platform shaker to generate an alternating fluid motion along the long axis of the slide flasks (Fig. 2C). Fast (50 rpm, equivalent to a fluid shear stress of 4.3 mPa, see (Zhou et al., 2010), 5 cm x 2 cm slide flask with 10 ml medium) and intermediate (25 rpm, 2.1 mPa) fluid motion led to the formation of unusually short myotubes with enlarged width and also larger multinucleate syncytia (Fig. 2G, H), while slow (12.5 rpm, 1.1 mPa) fluid motion had no obvious effect (Fig. 2I). Thus, in line with previous reports (Juffer et al., 2014; Jung, 2022), the specific type of fluid motion strongly influences the differentiation of myoblasts into myotubes: While unidirectional, steady, pulsatile and also interval flows suppress myotube formation even at very low rates (Juffer et al., 2014; Jung, 2022), an oscillating flow pattern, as shown here, apparently promotes myotube formation.

Discussion

In this study, we monitored the differentiation process of C2C12 murine myoblasts into multinucleate myotubes under clino-rotation. We found impaired myotube formation along a narrow band of approximately 4 mm width near the rotational axis, which previously has been interpreted as being caused by simulated microgravity conditions that are not present off-axis outside this band (Acharya et al., 2022; Brungs et al., 2016; Eiermann et al., 2013; Ivanova et al., 2011). However, an offset of the axis of rotation by 4 mm in additional experiments, which imposes a centrifugal force of 0.016 RCF, still impaired myotube formation along a narrow band near the centerline of the slide. We reasoned that the observed effects may not have been caused by the assumed microgravity but by rotation-induced fluid motion. Indeed, we found that myotube differentiation was also impaired by continuous fluid flow. In addition, we observed pronounced fluid motion in the rotating slide flasks, strongly suggesting that 2D-clinostats produce false-positive results that are misinterpreted as cellular microgravity responses.

Cell biological results from clino-rotation cannot be attributed to microgravity unless alternative explanations have been rigorously tested and excluded

For the vast majority of cell biology experiments, it will be prohibitively expensive to verify findings from ground-based simulated microgravity conditions in true microgravity in space/earth orbit. Therefore, a particularly thorough and critical discussion of ground-based results is needed. Several authors have already cautioned that some findings obtained under simulated microgravity may in fact be attributed to confounding effects such as mechanical vibration or fluid motion (Herranz et al., 2013; Wüest et al., 2015; Wüest et al., 2017; Zhang et al., 2022). To address these concerns, the mechanical stress-sensitive dinoflagellate *Pyrocystis noctiluca* (NCBI:txid66792), known for its nocturnal bluish glow of breaking sea waves, was used as reporter for fluid motion and shear stress in a study designed primarily to compare the overall performance of different devices. *P. noctiluca* responded with less bioluminescence to 60 rpm 2D-clino-rotation than to random positioning. This result was interpreted to mean that a 2D-clinostat is a proven microgravity simulation device, characterised by negligible fluid motion or shear force (Hauslage et al., 2017). However, an apparent misinterpretation by later experimenters was, that a 2D-clinostat was suitable for studying microgravity effects in mammalian cells without the need to also test their flow and shear force sensitivity.

Our studies using tracer particles in 2D-clino-rotating slide flasks demonstrate substantial fluid motions and show that cellular responses to shear forces cannot be ruled out. Experimentally, our data confirm that suppressed C2C12 myotube formation is only present near a narrow band along the rotational axis during clino-rotation. This finding has been interpreted as i) that microgravity conditions supress myotube formation, and ii) that perfect microgravity conditions are only present within a 2 mm radius around the rotational axis. The latter interpretation is commonly accepted and strictly observed for sampling. For example, 1F6 human melanoma cells (Fontijn et al., 2009; Van Muijen et al., 1991) grown in slide flasks and 2D-clino-rotated at 60 rpm for 24h showed significantly reduced guanylyl cyclase A mRNA levels limited to samples taken from the inner 6 mm wide axial area (Eiermann et al., 2013). Moreover, ML-1 (Schönberger et al., 2000) and RO82-W-1 (Estour et al., 1989) follicular thyroid cancer cells grown in slide flasks and 2D-clino-rotated at 60 rpm for either 3 or 7 days showed marked formation of actin stress fibres and subplasmalemmal enrichment of F-actin within the inner 6 mm wide axial area (Svejgaard et al., 2015). Another comprehensive study using spontaneous-beating cardiomyocytes generated from human-induced pluripotent stem cells grown in custom-modified slide flasks and 2D-clino-rotated at 60 rpm for 2 days showed multiple mitochondria-, contraction-, and senescence-related alterations and dysfunctions in samples taken from the inner 3 mm wide axial area. Notably, this study also reported the formation of actin stress fibres and sarcolemmal caveolae

in the 2D-clino-rotated cardiomyocytes as a clear indication of the presence of mechanical stress (Acharya et al., 2022).

However, the common notion that cellular effects attributed to the theoretically assumed microgravity are confined only to a narrow region close to the rotational axis is contradicted by our findings. In particular, when we rotated our slides eccentrically 4 mm off-axis, we still observed the same narrow band of reduced myotube formation. Impaired myotube formation was also reported for 60 rpm 3D-clino-rotation of differentiating C2C12 myoblasts (Calzia et al., 2020), where the 2-axis rotation is known to cause substantial fluid motion and shear stress (Wüest et al., 2017; Zhang et al., 2022). Considering that fluid motion is a potent stimulator of numerous cell responses, which we also demonstrate in our present study, previously published results obtained with clinostats in combination with adherent mammalian cells, a selection of which has been cited here, need to be re-interpreted. While we do not question the validity of the reported data, we caution that the reported cellular effects observed in clinostats are most likely not due to simulated microgravity but rather to fluid flow effects.

A recent study compared myotubes that were pre-formed from L6 rat myoblasts (ATCC CRL-1458) and subsequently exposed to i) real microgravity and a 1 xg control condition produced by centrifugation in the space station and to ii) ground-based simulated microgravity using random-mode 3D-clino-rotation and a static, non-rotating 1 xg control condition (Uchida et al., 2018). The study reported reduced myotube diameters after 10 days in real microgravity and after 3 days in random-mode 3D-clino-rotation. However, as presented (but not discussed) in the study, the ground-based, static, non-rotating, 'true 1 xg control' and the '1 xg centrifugation control' in the space station resulted in markedly different myotube diameters (see figure 2A,B in (Uchida et al., 2018)). Thus, we argue that based on the different effects of the two experimental 1 xg controls, the similar, however, comparably much smaller reductions of myotube diameters under real space versus simulated ground-based microgravity conditions cannot be straight-forwardly compared and most likely have different underlying mechanisms.

Strategies for improved experimental design

To identify spurious cellular responses caused by effects other than the desired simulated microgravity, further control experiments in addition to static, non-rotating cell samples must be included, for example offset-rotating controls as used in the present work, or a vertical-rotating control (see supplementary figure 1 in (Li et al., 2022)). A vertical-rotating control introduces in addition a new cell culture condition in the form of a gravitational vector in-plane with the cell-matrix interface, as

compared to a normal-acting force vector under standard culture conditions, and therefore requires a corresponding vertical static, non-rotating culture as a further control. Additionally, other controls to assess the effects of fluid motion need to be included. In this respect, the individual sensitivity of the specific cell type used must also be tested, as it can vary markedly (between e.g., protist vs. insect vs. mammalian cell, primary vs. immortalized cell, fibroblast vs. myoblast vs. endothelial cell, etc.).

Further, it is paramount to reduce or altogether prevent the intrinsic, rotation-induced fluid flow. To accomplish this, it is first necessary to understand the cause of the fluid moving in a 2D-clinostat, which is not obvious. In fact, previous fluid dynamic modelling suggested that the culture medium in a 2D-clino-rotating culture flask becomes steady after an initial phase of motion (Wüest et al., 2017), so that cultured cells would not be exposed to shear forces. However, this is only true for ideal conditions, in particular for a perfectly steady rotational speed, and for a perfectly steady axis of rotation. In practice, small fluctuations of the drive motor, combined with small oscillatory lateral movements due to the eccentric rotation of the side flasks, will inevitably cause fluid motion due to inertial and Coriolis forces.

A first, simple strategy is therefore to reduce the circulating fluid mass by reducing the height of the slide flask or other culture vessel, but this would require a gas-permeable flask material and further poses limits to the duration of the experiment before the cell culture medium needs to be exchanged. One option would be to use quite small culture vessels, such as channel slides, in which the medium is cyclically exchanged at larger time intervals, presumably on an hourly, half-day or daily scale, by connected pumps and reservoirs. However, vessels of very small dimensions can also influence the cells to be investigated, so that the influence of the geometry of the vessels and their surface properties, including any applied surface micropatterning, would also have to be taken into account. Another strategy could be to increase the viscosity of the cell culture medium. This would reduce the speed of fluid motion, but at the same time the positive effect could be cancelled as the fluid shear stress at the cell surface increases in proportion to the viscosity. The latter problem could be avoided by completely filling the culture vessel with an elastic hydrogel as culture medium. This hydrogel would need to be sufficiently permeable for gas exchange and nutrient transport. Possible examples are inert biopolymer-based hydrogels on the basis of alginate or agarose. Furthermore, matrix protein-based hydrogels containing e.g., collagen, fibrin, or Matrigel could offer the possibility to explore cell or microtissue behaviour under true 3D-culture conditions in combination with simulated microgravity. At the same time, the technical design of a clinostat must be improved to minimize rotational speed fluctuations and to maximize the stability of the rotational axes.

But even with a perfect design that completely prevents fluid flow and shear forces, experimenters should question the assumption that microgravity-like conditions can be achieved by averaging-out the vector of gravity. For example, bone cells strongly respond to oscillatory fluid shear stress even

when the stress has a time-average of zero (Ponik et al., 2007). On an even more fundamental level, researches should also question the assumption that gravitational forces are of relevant magnitude to be sensed by a single cell in a near-buoyant, aqueous environment. Considering that C2C12 cells as used in this study generate traction stresses of typically 1 kPa or more (Sakar et al., 2012), normal gravitational stresses acting at the cell-matrix interface are more than 5 orders of magnitude smaller. In fact, the total gravitational forces of a single cell in water of around 1 to 2 pN (assuming a cell density of 1.05 g/cm^3) is smaller than the contractile force generated by a single myosin molecule. Thus, apart from the unsolved technical challenges, the problem of separating the cellular effects of these extremely small gravitational forces from the combined effects of much larger contractile, thermal, and fluid forces or geometric constrains remains to be addressed. This might be done by extensive transcriptomic or proteomic analyses of samples derived from true microgravity, simulated microgravity, fluid flow, vibration, and other assays, and a multiple comparison of the resulting omics-patterns. Consideration of the here discussed strategies for improved assay design requires further studies and inevitably makes the interpretation of results more complex.

Methods

Exposure of differentiating C2C12 muscle cells to 2D-clino-rotation and fluid motion

C2C12 myoblasts derived from C3H mouse skeletal muscle (ECACC 91031101, also available as ATCC CRL-1772) with low passage number (highly myogenic passage no. 6 at start of this work) were grown in DMEM supplemented with 10% fetal calf serum, 2 mM L-glutamine, 1 mM pyruvate, 1x non-essential amino acids, 100 U/ml penicillin, and 0.1 mg/ml streptomycin (all from Pan Biotech, Aidenbach, Germany) in a NuAir incubator (NU-5841E; ibs tecnomara GmbH, Fernwald, Germany) at 5% CO_2 and 37°C. Semi-confluent cultures were split using 0.05% trypsin/0.5 mM EDTA (Pan Biotech, Aidenbach, Germany) by 1:8 for assays in SlideFlasks (#170920; Nunc/Thermo Scientific, Waltham, USA) or 1:20 for maintenance in standard 100 mm culture dishes (#83.3902; Sarstedt, Nümbrecht, Germany). Differentiation of the myoblasts into myotubes was induced by replacing the growth medium with a low-mitotic medium, i.e., the former growth medium with the fetal calf serum replaced by 5% horse serum (Gibco/Thermo Scientific, Waltham, USA). The used horse serum was from a batch that had been tested regarding muscle cell differentiation. Myotube formation was monitored up to 8 days.

For exposure to clino-rotation, C2C12 myoblasts were grown to confluency in slide flasks within 1 day after splitting, and immediately after addition of differentiation medium clino-rotation was done for 6

days. The culture vessels were attached to a custom-made slide flask-2D-clinostat (Eiermann et al., 2013; Mansour Jamaleddine, 2021) shelved in the above-mentioned incubator at 5% CO_2 and 37°C (Fig. 1A-C); static, non-rotating control slide flasks were placed on top of the clinostat to rule out the possibility of effects of the unavoidable device vibration (Fig. 1A). Rotation speed was 60 rpm (360 deg/s, 6.3 rad/s) generating few millimetres wide central band-formed areas of centrifugal acceleration, for example (band width, acceleration, fraction of Earth's gravity): 3 mm, 0.059 m/s², 0.006 RCF; 4 mm, 0.079 m/s², 0.008 RCF; 6 mm, 0.118 m/s², 0.012 RCF; 8 mm, 0.158 m/s², 0.016 RCF; 12 mm, 0.237 m/s², 0.024 RCF; 16 mm, 0.316 m/s², 0.032 RCF; 18 mm, 0.355 m/s², 0.036 RCF. In addition, sets of culture vessels were attached in way that the slide was positioned 4 mm above the rotational axis; this was achieved by holding clamps with a thicker intermediate base (Fig. 1B, blue clip vs. black clip, and axis of rotation label in yellow). Clino-rotation experiments were independently performed three times with four slide flasks for each condition (clino-rotation, offset-rotation, static non-rotating control). All images and data are from cells located within a central 4 mm wide area along the rotational axis across the entire slide. Clino-rotating slide flasks were completely filled with incubator-equilibrated medium, carefully sealed with Parafilm M (Bemis, Neenah, USA) and the screw caps, and checked for total absence of air bubbles during the entire duration of the experiment. All 'Bonn criteria' for a clinostat device (Hammond and Allen, 2011) are covered by parameters specified in the two above paragraphs.

For 5 to 7 days exposure to unidirectional flow, C2C12 myoblasts in custom-modified slide flasks, termed 'flow flasks' (Jung, 2022), were grown to confluency within 1 day after splitting. Immediately after addition of differentiation medium, culture vessels were connected to peristaltic pumps (Pump-P1; Pharmacia Biotech AB, Uppsala, Sweden) using 2 mm inner diameter PBS-washed and autoclaved silicone tubes (Fig. 2B). Flow rate was set to either 10x10 (5.7 mL/min), 1x10 (570 µL/min), or 1x1 (57 µL/min); exact flow rates were determined by measuring 1-minute-flow volumes at the end of each experiment. Flow experiments were independently performed three times (one flow setting per experiment) with four slide flasks for each condition (flow and static control). Images were obtained from cells located within a central 4 mm wide area across the entire long axis of the slide.

For 5 to 7 days exposure to oscillating flow along the long axis of slide flasks, C2C12 myoblasts were also grown to confluency within 1 day after splitting. Immediately after the addition of differentiation medium, the slide flasks were centrally placed on a 5°-tilt-angle rocking platform shaker (Duomax 1030; Heidolph, Kelheim, Germany) (Fig. 2C). Rocking rate was set to either fast (50 rpm), medium (25 rpm), or slow (12.5 rpm) and verified by counting the 1-minute-number of cycles. Rocking experiments were independently performed three times (one rocking rate per experiment) with three

slide flasks for each condition (rocking and static control). Images were obtained from cells located within a central 4 mm wide area across the entire long axis of the slide.

Microscopic imaging, fluid motion monitoring, and data analysis

Microscopic images were recorded with a transmission light microscope (DMIL LED; Leica Microsystems, Wetzlar, Germany), objective HI PLAN I 10x/0.22 PH1, equipped with a heated stage (Tempcontrol-37; Pecon, Erbach, Germany) and stand-alone FLEXACAM C1 colour camera (Leica Microsystems, Wetzlar, Germany). Using the phase contrast images in random order, myotubes were independently assessed and counted by two expert authors of this study. The widths of these myotubes was measured at their position of maximal width and respective diameters were determined using ImageJ v.1.53 (Schneider et al., 2012). Statistical analysis was performed using Prism v.6.07 (GraphPad Software Inc., San Diego, USA); data passed D'Agostino & Pearson omnibus normality testing, and statistical significances were calculated using one-way ANOVA with Tukey's multiple comparisons correction and subsequent unpaired two-tailed Student's t-tests. Data are shown as scatter dot plots with medians and interquartile ranges. For fluid motion monitoring, a mini-camera (no brand, 640x480 pixel resolution at 10 fps) complemented with an objective (Olympus, 4x/0.10, CX22 PL4X) was fixed facing the front side of a slide flask (Fig. 3A). Video frame snapshots were created using VLC media player v.3.0.18 (VideoLAN Organization) and used to manually generate single-bead-tracks. Supplementary video clips were generated using ClickPoints (Gerum et al., 2016). Images were processed and figures assembled using CorelDraw Graphics Suite X7 (Corel Corporation, Ottawa, Canada).

Declarations

Funding

This research did not receive any specific grant from funding agencies in the public, commercial, or not-for-profit sectors.

Competing interests

The authors declare that they have no competing interests.

Authors' contributions

J.M., C.B., and C.S.C. jointly conceived the study, reviewed data, designed figures, and drafted the manuscript. J.M., C.B., M.J., and C.S.C. designed and carried out experiments and analysed data. J.M. and C.S.C. performed statistical evaluations. L.E., B.F., and C.S.C. analysed data, reviewed data, and jointly finalised the manuscript; C.S.C. prepared the final version of manuscript figures. All authors have read and agreed to the final version of the manuscript.

Acknowledgements

We gratefully acknowledge the following support of this work: Dr. Philip Born, Institute of Materials Physics in Space, German Aerospace Center, Cologne, Germany, for providing polystyrene beads; Mr. Sebastian Steinhäuser and Dr. Thomas Voigtmann, Institute of Materials Physics in Space, German Aerospace Center, Cologne, Germany, for helpful discussions of fluid motion profiles; Dr. Peter van der Ven, Institute for Cell Biology, University of Bonn, Germany, for providing horse serum from a batch that had been tested for C2C12 muscle cell differentiation; and last but not least Mr. Marvin Diegeler, Photo Services Cologne, German Aerospace Center, Cologne, Germany, for professional photography of experimental setups.

Data availability

The data that support the findings of this study are available within the article and its supplementary material.

References

Acharya, A., Nemade, H., Papadopoulos, S., Hescheler, J., Neumaier, F., Schneider, T., Rajendra Prasad, K., Khan, K., Hemmersbach, R., Gusmao, E.G., Mizi, A., Papantonis, A., Sachinidis, A., 2022. Microgravity-induced stress mechanisms in human stem cell-derived cardiomyocytes. iScience 25, 104577.

Briegleb, W., 1992. Some qualitative and quantitative aspects of the fast-rotating clinostat as a research tool. ASGSB bulletin : publication of the American Society for Gravitational and Space Biology 5, 23-30.

Brungs, S., Egli, M., Wüest, S., Christianen, P.C.M., van Loon, J.J.W.A., Ngo-Anh, J., Hemmersbach, R., 2016. Facilities for Simulation of Microgravity in the ESA Ground-Based Facility Programme. Microgravity Science and Technology 28, 191-203.

Calvaruso, M., Militello, C., Minafra, L., La Regina, V., Torrisi, F., Pucci, G., Cammarata, F.P., Bravata, V., Forte, G.I., Russo, G., 2021. Biological and Mechanical Characterization of the Random Positioning Machine (RPM) for Microgravity Simulations. Life 11, 1190.

Calzia, D., Ottaggio, L., Cora, A., Chiappori, G., Cuccarolo, P., Cappelli, E., Izzotti, A., Tavella, S., Degan, P., 2020. Characterization of C2C12 cells in simulated microgravity: Possible use for myoblast regeneration. J. Cell. Physiol. 235, 3508-3518.

Eiermann, P., Kopp, S., Hauslage, J., Hemmersbach, R., Gerzer, R., Ivanova, K., 2013. Adaptation of a 2-D Clinostat for Simulated Microgravity Experiments with Adherent Cells. Microgravity Science and Technology 25, 153-159.

Estour, B., Van Herle, A.J., Juillard, G.J., Totanes, T.L., Sparkes, R.S., Giuliano, A.E., Klandorf, H., 1989. Characterization of a human follicular thyroid carcinoma cell line (UCLA RO 82 W-1). Virchows Arch. B. Cell Pathol. Incl. Mol. Pathol. 57, 167-174.

Fontijn, D., Bosch, L.J., Duyndam, M.C., van Berkel, M.P., Janmaat, M.L., Boven, E., 2009. Basic fibroblast growth factor-mediated overexpression of vascular endothelial growth factor in 1F6 human melanoma cells is regulated by activation of PI-3K and p38 MAPK. Cellular oncology : the official journal of the International Society for Cellular Oncology 31, 179-190.

Gerum, R., Richter, S., Fabry, B., Zitterbart, D.P., 2016. ClickPoints: an expandable toolbox for scientific image annotation and analysis. Methods Ecol Evol.

Hammond, T., Allen, P., 2011. The Bonn Criteria: Minimal Experimental Parameter Reporting for Clinostat and Random Positioning Machine Experiments with Cells and Tissues. Microgravity Science and Technology 23, 271-275.

Hasenstein, K.H., 2022. Blueprints for Constructing Microgravity Analogs. Methods Mol. Biol. 2368, 215-232.

Hauslage, J., Cevik, V., Hemmersbach, R., 2017. Pyrocystis noctiluca represents an excellent bioassay for shear forces induced in ground-based microgravity simulators (clinostat and random positioning machine). NPJ microgravity 3, 12.

Herranz, R., Anken, R., Boonstra, J., Braun, M., Christianen, P.C., de Geest, M., Hauslage, J., Hilbig, R., Hill, R.J., Lebert, M., Medina, F.J., Vagt, N., Ullrich, O., van Loon, J.J., Hemmersbach, R., 2013. Ground-based facilities for simulation of microgravity: organism-specific recommendations for their use, and recommended terminology. Astrobiology 13, 1-17.

Ivanova, K., Eiermann, P., Tsiockas, W., Hauslage, J., Hemmersbach, R., Gerzer, R., 2011. Natriuretic peptide-sensitive guanylyl cyclase expression is down-regulated in human melanoma cells at simulated weightlessness. Acta Astronaut. 7-8, 652-655.

Juffer, P., Bakker, A.D., Klein-Nulend, J., Jaspers, R.T., 2014. Mechanical loading by fluid shear stress of myotube glycocalyx stimulates growth factor expression and nitric oxide production. Cell Biochem. Biophys. 69, 411-419.

Jung, M., 2022. Optimizing culture conditions and ground controls of C2C12 myoblasts for FLUMIAS-ISS live-cell imaging microscope. Master thesis, University of Bonn, Germany.

Khodadadei, F., Liu, A.P., Harris, C.A., 2021. A high-resolution real-time quantification of astrocyte cytokine secretion under shear stress for investigating hydrocephalus shunt failure. Communications biology 4, 387.

Klaus, D.M., 2001. Clinostats and bioreactors. Gravitational and space biology bulletin : publication of the American Society for Gravitational and Space Biology 14, 55-64.

Lee, S., Kwok, N., Holsapple, J., Heldt, T., Bourouiba, L., 2020. Enhanced wall shear stress prevents obstruction by astrocytes in ventricular catheters. Journal of the Royal Society, Interface 17, 20190884.

Li, C., Pan, Y., Tan, Y., Wang, Y., Sun, X., 2022. PINK1-Dependent Mitophagy Reduced Endothelial Hyperpermeability and Cell Migration Capacity Under Simulated Microgravity. Frontiers in cell and developmental biology 10, 896014.

Liegibel, U.M., Sommer, U., Bundschuh, B., Schweizer, B., Hilscher, U., Lieder, A., Nawroth, P., Kasperk, C., 2004. Fluid shear of low magnitude increases growth and expression of TGFbeta1

and adhesion molecules in human bone cells in vitro. Exp. Clin. Endocrinol. Diabetes 112, 356-363.
Mansour Jamaleddine, J., 2021. Response of immortalized murine desminopathy myoblasts to altered gravitational loading. Bachelor thesis, University of Bonn, Germany.
Ponik, S.M., Triplett, J.W., Pavalko, F.M., 2007. Osteoblasts and osteocytes respond differently to oscillatory and unidirectional fluid flow profiles. J. Cell. Biochem. 100, 794-807.
Rittweger, J., Albracht, K., Fluck, M., Ruoss, S., Brocca, L., Longa, E., Moriggi, M., Seynnes, O., Di Giulio, I., Tenori, L., Vignoli, A., Capri, M., Gelfi, C., Luchinat, C., Francheschi, C., Bottinelli, R., Cerretelli, P., Narici, M., 2018. Sarcolab pilot study into skeletal muscle's adaptation to long-term spaceflight. NPJ microgravity 4, 18.
Sakar, M.S., Neal, D., Boudou, T., Borochin, M.A., Li, Y., Weiss, R., Kamm, R.D., Chen, C.S., Asada, H.H., 2012. Formation and optogenetic control of engineered 3D skeletal muscle bioactuators. Lab on a chip 12, 4976-4985.
Schneider, C.A., Rasband, W.S., Eliceiri, K.W., 2012. NIH Image to ImageJ: 25 years of image analysis. Nat. Methods 9, 671-675.
Schönberger, J., Bauer, J., Spruss, T., Weber, G., Chahoud, I., Eilles, C., Grimm, D., 2000. Establishment and characterization of the follicular thyroid carcinoma cell line ML-1. J Mol Med (Berl) 78, 102-110.
Svejgaard, B., Wehland, M., Ma, X., Kopp, S., Sahana, J., Warnke, E., Aleshcheva, G., Hemmersbach, R., Hauslage, J., Grosse, J., Bauer, J., Corydon, T.J., Islam, T., Infanger, M., Grimm, D., 2015. Common Effects on Cancer Cells Exerted by a Random Positioning Machine and a 2D Clinostat. PloS one 10, e0135157.
Uchida, T., Sakashita, Y., Kitahata, K., Yamashita, Y., Tomida, C., Kimori, Y., Komatsu, A., Hirasaka, K., Ohno, A., Nakao, R., Higashitani, A., Higashibata, A., Ishioka, N., Shimazu, T., Kobayashi, T., Okumura, Y., Choi, I., Oarada, M., Mills, E.M., Teshima-Kondo, S., Takeda, S., Tanaka, E., Tanaka, K., Sokabe, M., Nikawa, T., 2018. Reactive oxygen species upregulate expression of muscle atrophy-associated ubiquitin ligase Cbl-b in rat L6 skeletal muscle cells. Am. J. Physiol. Cell Physiol. 314, C721-C731.
Van Muijen, G.N., Cornelissen, L.M., Jansen, C.F., Figdor, C.G., Johnson, J.P., Brocker, E.B., Ruiter, D.J., 1991. Antigen expression of metastasizing and non-metastasizing human melanoma cells xenografted into nude mice. Clin. Exp. Metastasis 9, 259-272.
Wakida, N.M., Cruz, G.M.S., Pouladian, P., Berns, M.W., Preece, D., 2020. Fluid Shear Stress Enhances the Phagocytic Response of Astrocytes. Frontiers in bioengineering and biotechnology 8, 596577.
Wüest, S.L., Richard, S., Kopp, S., Grimm, D., Egli, M., 2015. Simulated microgravity: critical review on the use of random positioning machines for mammalian cell culture. BioMed research international 2015, 971474.
Wüest, S.L., Stern, P., Casartelli, E., Egli, M., 2017. Fluid Dynamics Appearing during Simulated Microgravity Using Random Positioning Machines. PloS one 12, e0170826.
Zhang, Y., Richards, J.T., Hellein, J.L., Johnson, C.M., Woodall, J., Sorenson, T., Neelam, S., Ruby, A.M.J., Levine, H.G., 2022. NASA's Ground-Based Microgravity Simulation Facility. Methods Mol. Biol. 2368, 281-299.
Zhou, X., Liu, D., You, L., Wang, L., 2010. Quantifying fluid shear stress in a rocking culture dish. J. Biomech. 43, 1598-1602.

Figure legends

Figure 1. Suppression of myotube formation during clino-rotation does not depend on simulated microgravity. (**A**) View into the opened cell culture incubator with part 1 of the experimental setup. In the background, the slide flask 2D-clinostat with several slide flasks containing confluent layers of C2C12 myoblasts attached to the rotation axes and filled with differentiation medium. On top of the device the static, non-rotating controls. In the foreground, two peristaltic pumps with connected slide flasks converted into flow flasks by means of grommets attached to the end faces. (**B**) Detailed view of two slide flasks attached with clamps to the rotation axes of the clinostat to illustrate their usual position for clino-rotation (upper flask, black clip) compared to the additional position of offset-rotation (lower flask, blue clip) used to demonstrate side effects of the rotation in this study. Upper yellow line, position of the rotation axis in plane with the slide. Lower yellow line, offset-rotation with the rotation axis 4 mm below the slide with the adherent cells (arrow). (**C**) Slightly enlarged view of (B) during the 60 rpm-rotation of the slide flasks. (**D-F**) Phase contrast microscopic views of C2C12 cells from the central 4 mm wide area along the rotation axis of slide flasks after 6 days of differentiation into multinucleate myotubes during (D) continuous clino-rotation, (E) continuous 4 mm offset-rotation or from (F) static, non-rotating controls. Arrowheads, examples of the formed myotubes. Asterisks, areas where myoblasts remained prominent. (**G**) Quantitation of the number of formed myotubes after 6 days of differentiation under clino-rotation, offset-rotation or static control condition. Shown is the representative result of one of a total of three independent experiments. Myoblasts of eight microscopic views from the 4 mm wide area along the central axis of rotation across the entire slide of each slide flask were counted from four slide flasks per condition of the experiment shown. Note that there is no significant difference between clino-rotation and offset-rotation, but both conditions differ significantly from the static, non-rotating control. (**H**) Quantification of the width of the myotubes counted in (G), each measured at the point of the largest diameter. The marginal differences in diameter are not considered biologically relevant, and therefore significances are given in brackets. (G, H) Scatter dot plots with medians (values are indicated) and interquartile ranges. Statistical significances calculated by Student's t-test subsequent to normality and homoscedasticity as well as one-way ANOVA testing.

Figure 2. Fluid motion markedly influences C2C12 myotube formation. (**A**) Tests with the addition of 500 µm diameter polystyrene tracer particles to slide flasks filled with medium demonstrate the possible presence of a cylindrical fluid motion during 2D-clino-rotation. (**B**) Enlarged view of the two peristaltic pumps with the flow flasks connected. (**C**) Slide flasks containing confluent layers of C2C12 myoblasts and differentiation medium are placed on a 5°-tilt-angle rocking platform; non-rocking

controls are located to the right of the device. (**D**-**F**) Phase contrast microscopic views of C2C12 cells from the central area of flow flasks perfused with differentiation medium at flow rates of 5.7 mL/min (D), 570 µL/min (E), and 57 µL/min (F) after 6 days of differentiation. The unidirectional medium flow markedly inhibits myotube formation. Hashtags, areas with formation of a few myotubes at lower flow rates. (**G**-**I**) Phase contrast microscopic views of C2C12 cells from the central area of slide flasks filled with differentiation medium and 5°-tilt-angle rocked at 50 rpm (G), 25 rpm (H), and 12.5 rpm (I). Six days of differentiation under fast to moderate, alternating fluid motion result in the formation of unusually short and wide myotubes; hashtags, large and multinucleate syncytia.

Figure 3. Fluid motion within 2D-clino-rotating slide flasks. (**A**) View of the experimental setup for documenting fluid motion in a slide flask during 2D-clino-rotation. In line from left to right, slide flask filled with differentiation medium and polystyrene tracer particles, a 4x plan objective, a mini-camera (640x480p, 10fps), and a power bank. (**B**) Compilation of the observed flow directions and velocities during the steady-state phase of 2D-clino-rotation. Background image, exemplary camera view (video snapshot) in longitudinal axis of the slide flask; multiple tracer particles are visible. Grey straight and circular arrows, position and direction of mainly occurring flows (up, down, horizontal, circular) observed with 250 µm or 500 µm whitish-transparent and a few blackened tracer particles. Coloured and numbered dots, tracks of representative individual particles with indication of their mean trajectory velocities. Yellow marker, position of the rotational axis at the slide and rotation direction. A total of 83 video sequences were evaluated; an exemplary video clip is available in the supplement (Video S1). Note that since the fluid shear rate (the gradient of the fluid flow velocity) is low in the bulk of the medium, the fluid motion is not measurably perturbed by the presence of the beads.

Supplementary materials

Supplementary video 1. Fluid motion within 2D-clino-rotating slide flasks. Exemplary video clip documenting marked fluid motion in a slide flask during the steady-state phase of 2D-clino-rotation. Multiple such video clips were used to compile the complex pattern of observed flow directions and velocities as shown in figure 3.

1

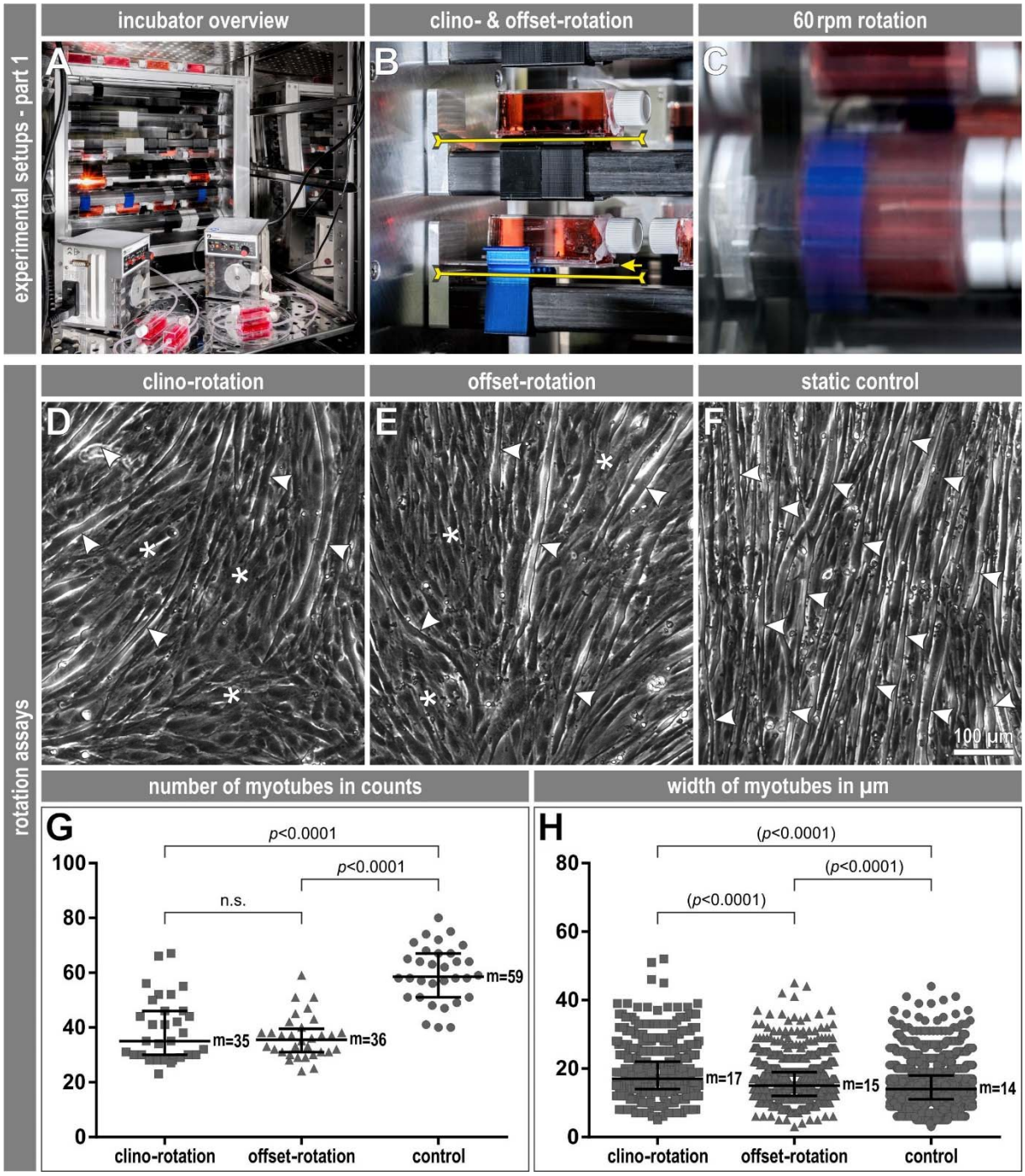
experimental setups - part 1
incubator overview
clino- & offset-rotation
60 rpm rotation
A
B
C
rotation assays
clino-rotation
offset-rotation
static control
D
E
F
100 µm
number of myotubes in counts
width of myotubes in µm
G
p<0.0001
p<0.0001
n.s.
m=35
m=36
m=59
clino-rotation
offset-rotation
control
H
(p<0.0001)
(p<0.0001)
(p<0.0001)
m=17
m=15
m=14
clino-rotation
offset-rotation
control

2

3

Figure 1

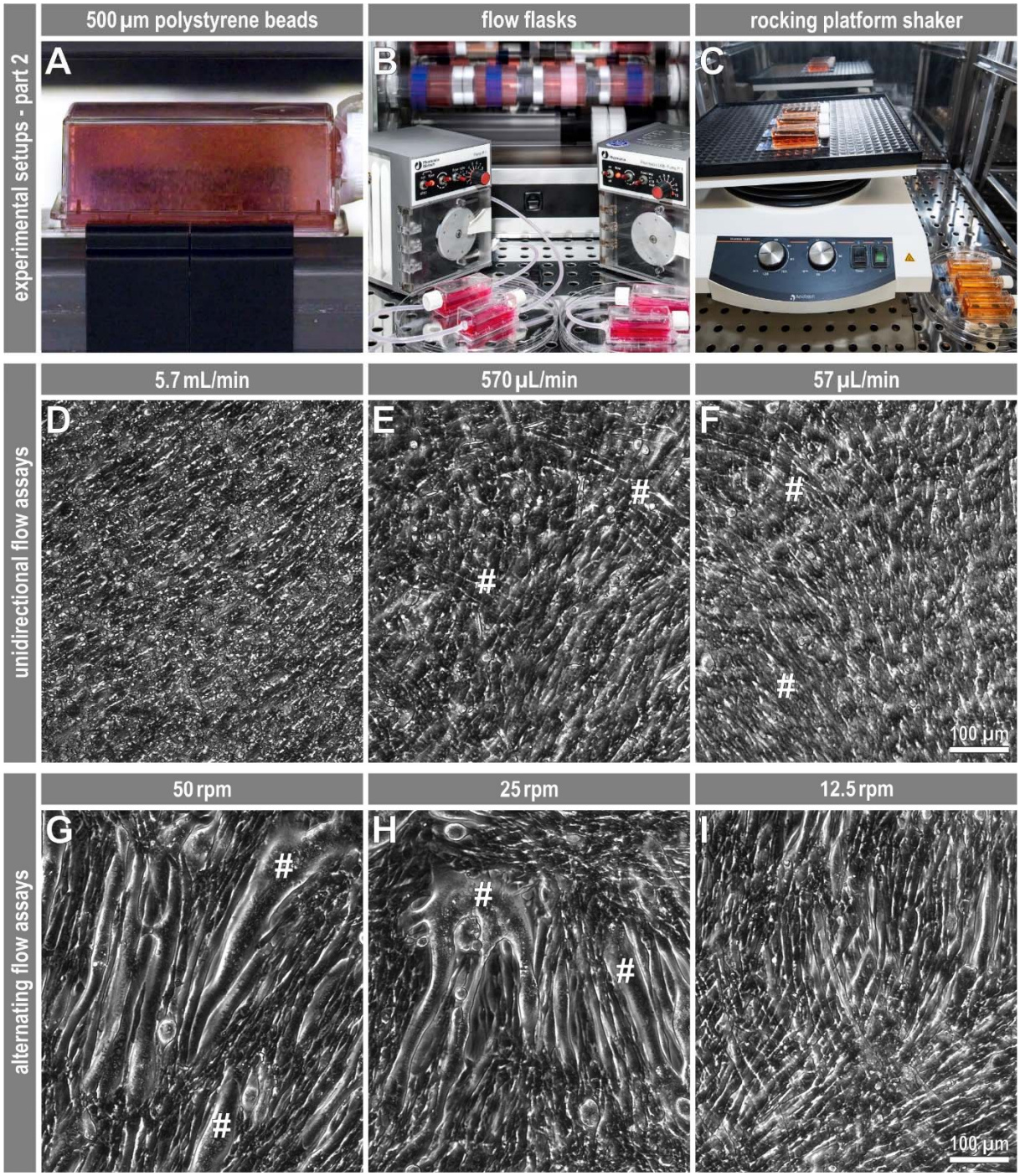
experimental setups - part 2
500 µm polystyrene beads
flow flasks
rocking platform shaker
A
B
C
unidirectional flow assays
5.7 mL/min
570 µL/min
57 µL/min
D
E
F
#
100 µm
alternating flow assays
50 rpm
25 rpm
12.5 rpm
G
H
I
100 µm

Figure 2

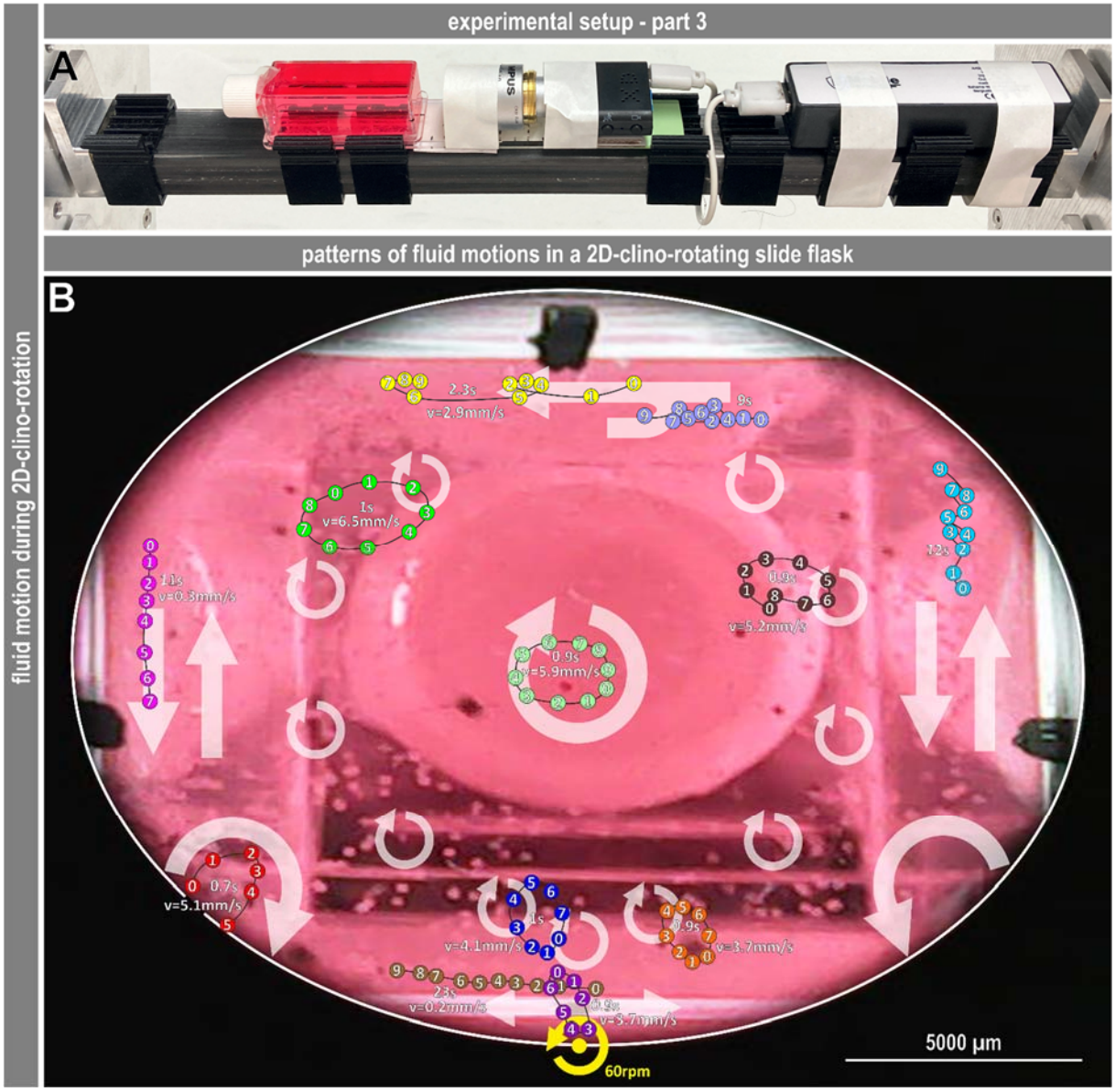
fluid motion during 2D-clino-rotation
experimental setup - part 3
A
patterns of fluid motions in a 2D-clino-rotating slide flask
B
2.3s
v=2.9mm/s
9s
1s
v=6.5mm/s
1.1s
v=0.3mm/s
0.9s
v=5.2mm/s
12s
0.9s
v=5.9mm/s
0.7s
v=5.1mm/s
1s
v=4.1mm/s
0.9s
v=3.7mm/s
2.5s
v=0.2mm/s
0.9s
v=3.7mm/s
60rpm
5000 µm

Figure 3